NEW FORMULAE BASED ON FOURIER EXTENSION FOR BEARINGLESS SWITCHED RELUCTANCE MOTORS

Ye Shuang* Deng Zhiquan Yan Yangguang
Dept. of Automatic Control, Nanjing University of Aeronautics and Astronautics,
Nanjing, 210016 P.R.C
*ye_shuang@yahoo.com

ABSTRACT

In this paper, new formulae based on Fourier analysis for bearingless switched reluctance motors have been proposed. Two main winding modes are compared and the motor has been analyzed by using ANSYS. Expression obtained through Fourier extension is differentiable and is also effective in general switched reluctance motors supported by mechanical bearings.

INTRODUCTION

Switched reluctance motors have been the focus of extensive research efforts because of their inherent advantageous features such as fault-tolerance, robustness, low cost and possible operations in high temperatures [1].

Air gap length in switched reluctance motors is reduced compared to other machines, which lead to significant amount of magnetic attraction generated in the radial direction. Bearingless switched reluctance motors may possibly take advantage of this inherent large magnetic attraction for rotor shaft magnetic suspension. The theoretical equations of radial forces and control schematic have been derived [2] [3].

Because of its doubly salient structure, it is not possible to obtain an exact analytical model for switched reluctance motor. Numerous authors have addressed this problem with solutions ranging from finite element analysis to flux tube. The method of extending a simplified inductance expression in Fourier series has been proposed [4].

This paper presents new formulae for radial forces based on Fourier analysis of the permeance. Finite element analysis is employed here to emendate the expressions of permeance and to examine the accuracy of the expression of radial force.

MOTOR CONFIGURATION

A motor is designed for further analysis such as finite element analysis. Fig.1 illustrates a 3-phase, 12/8 pole motor discussed in this paper. A summary of important required input design parameters are given in TABLE 1.

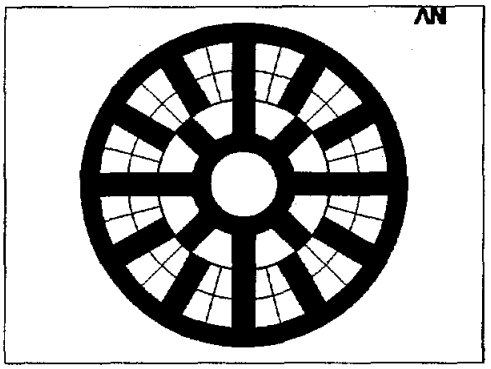

FIGURE.1 Structure of the motor

TABLE 1: Main dimensions

Stack length, h	95mm

Average air-gap length, l_0	0.25mm
Stator poles arc coefficient, β_s	0.5
Number of stator poles, N_s	12
Rotor poles arc coefficient, β_r	0.3333
Number of rotor poles, N_r	8
Stator outer diameter	145mm
Rotor pole radius, r	38.25mm
Number of turns of main winding, N_m	22
Number of turns of radial force winding, N_b	18

The principle of radial force production has been proposed in [2]. In α -direction, main winding generates a biasing flux, whose flux density is increased at one air gap and decreased at the other air gap by radial force winding separately, and thus an imbalance of flux density causes the generation of F_α. F_α and F_β, produced by two independent radial force windings, will produce radial force of any direction expected.

Because of the independent operation of different phases [3], only A-phase magnetic equivalent circuit is used to have a simple calculation in this paper. The main winding of one phase in [2] is connected in NSNS mode clockwise, as shown in Fig.2 (a). Main windings are in gray while radial force windings are in white. In Fig.2 (b), another mode: NNSS, which includes two sub-modes, is also shown. Both modes will be able to generate radial force and their performances will be compared in terms of simplicity and inductances.

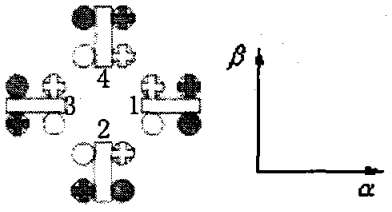

FIGURE.2 (a): Illustration of NSNS

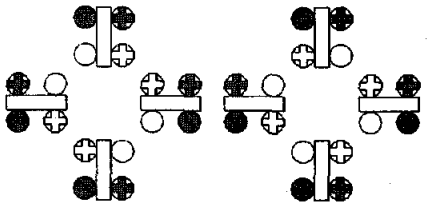

FIGURE.2 (b): Illustration of NNSS_a & NNSS_b

DERIVATION OF NEW FORMULAE FOR INDUCTANCES

Fourier Analysis of Permeance

The following assumptions are considered in calculation:

1 Magnetic saturation can be neglected

2 The rotor displacement is small enough compared with the air-gap length

3 Only flux paths that link both stator and rotor are considered.

The principle of Fourier analysis is to extend a simplified sectionalized expression (which describe the mathematical relationship rather coarsely) in Fourier series to obtain continuous expression. The simplified model of permeance under each pole for extension can be written as,

$$P_a(\theta)=\begin{cases} P_{\min} & \frac{-\theta_r}{2}<\theta<\frac{-\theta_r}{2}+\theta_1 \\ P_{\min}+slope(\theta-(\theta_1-\frac{\theta_r}{2})) & \frac{-\theta_r}{2}+\theta_1<\theta<0 \\ P_{\min}-slope(\theta-(\frac{\theta_r}{2}-\theta_1)) & 0<\theta<\frac{\theta_r}{2}-\theta_1 \\ P_{\min} & \frac{\theta_r}{2}-\theta_1<\theta<\frac{\theta_r}{2} \end{cases} \quad (1)$$

$$\theta_1=\frac{\theta_r}{2}(1-\beta_s\frac{N_r}{N_s}-\beta_r) \quad (2)$$

$$\theta_2=\frac{\theta_r}{2}(1+\beta_s\frac{N_r}{N_s}-\beta_r) \quad (3)$$

$$\theta_r=\frac{2\pi}{N_r} \quad (4)$$

$$slope=\frac{P_{\max}-P_{\min}}{\theta_2-\theta_1} \quad (5)$$

$$P_{\max} = \frac{\mu_0 A_n}{l_0} \tag{6}$$

Where A_n is the area of rotor pole.

$P_{\min}$ has been obtained in [2], in case that $\theta_a = \frac{\pi}{12}$, c=1.49, thus,

$$P_{\min} = \frac{4\mu_0 h}{\pi} \ln(\frac{\frac{cr}{3} + l_0}{l_0}) \tag{7}$$

The Fourier Extension of the model can be written as,

$$P_a = A\ln(\frac{cr}{3l_0}+1) + \frac{B}{l_0} + [C\ln(\frac{cr}{3l_0}+1) + \frac{D}{l_0}] \bullet \sum_{k=1}^{\infty} \frac{\sin^2(\frac{\pi k N_r}{24})}{k^2} \cos(kN_r\theta) \tag{8}$$

Substituting $l_0 \pm \alpha$ and $l_0 \pm \beta$ into l_0 in (8), we will get $P_{a1} \sim P_{a4}$.

Derivation of Inductances

The relationship of NSNS mode between permeance and inductance has been proposed in [3]. The relationship of NNSS mode can be derived similarly, but in 2 sub-modes: NNSS_a and NNSS_b as,

NNSS_a:

$$L_{ma} = \frac{4N_m^2(P_{a1}+P_{a4})(P_{a2}+P_{a3})}{P} \tag{9.a}$$

$$L_{sa1} = L_{sa2} = \frac{N_b^2(P_{a1}+P_{a3})(P_{a2}+P_{a4})}{P} \tag{10.a}$$

$$M_{(ma,sa1)} = \frac{2N_m N_b(P_{a1}P_{a2} - P_{a3}P_{a4})}{P} \tag{11.a}$$

$$M_{(ma,sa2)} = -\frac{2N_m N_b(P_{a1}P_{a2} - P_{a3}P_{a4})}{P} \tag{12.a}$$

$$M_{(sa1,sa2)} = -\frac{N_b^2(P_{a1}+P_{a3})(P_{a2}+P_{a4})}{P} \tag{13.a}$$

NNSS_b:

$$L_{ma} = \frac{4N_m^2(P_{a1}+P_{a4})(P_{a2}+P_{a3})}{P} \tag{9.b}$$

$$L_{sa1} = \frac{N_b^2(P_{a1}+P_{a3})(P_{a2}-P_{a4})}{P} \tag{10.b}$$

$$L_{sa2} = -\frac{N_b^2(P_{a1}+P_{a3})(P_{a2}-P_{a4})}{P} \tag{11.b}$$

$$M_{(ma,sa1)} = M_{(ma,sa2)} = \frac{2N_m N_b(P_{a1}P_{a2} + P_{a3}P_{a4} + 2P_2P_4)}{P} \tag{12.b}$$

$$M_{(sa1,sa2)} = \frac{N_b^2(P_{a1}+P_{a3})(P_{a2}-P_{a4})}{P} \tag{13.b}$$

where P is a sum of $P_{a1} \sim P_{a4}$.

We know that in the case that the radial rotor position is stably controlled, i.e., $\alpha = \beta = 0$, $P_{a1} = P_{a2} = P_{a3} = P_{a4} = \frac{P}{4}$, we'll get,

TABLE 2: Comparison of the two modes

	NSNS	NNSS_a	NNSS_b
L_{ma}	$N_m^2 P$	$N_m^2 P$	$N_m^2 P$
L_{sa1}	$\frac{N_b^2 P}{2}$	$\frac{N_b^2 P}{4}$	0
L_{sa2}	$\frac{N_b^2 P}{2}$	$\frac{N_b^2 P}{4}$	0
$M_{(ma,sa1)}$	0	0	$\frac{N_m N_b P}{2}$
$M_{(ma,sa2)}$	0	0	$\frac{N_m N_b P}{2}$
$M_{(sa1,sa2)}$	0	$-\frac{N_b^2 P}{4}$	0

Table 2 says that there are two sub-modes according to actual radial force requirement, which makes the construction of theoretical model very difficult. It can be noticed that mutual inductance between the two radial force windings in NNSS_a is not so small as to be neglected, which means strong coupling of the two radial force windings. Thus, it will be rather difficult to control F_α and F_β independently.

It can be concluded that NSNS mode is more preferable. And the following derivation is based on NSNS mode.

Substituting $P_{a1} \sim P_{a4}$ in the equations of NSNS mode in [2], the inductances are given as,

$$L_{ma} = 4N_m^2\{A\ln(\frac{cr}{3l_0}+1)+\frac{B}{l_0} + [C\ln(\frac{cr}{3l_0}+1)+\frac{D}{l_0}]\sum_{k=1}^{\infty}\frac{\sin^2(\frac{\pi kN_r}{24})}{k^2}\cos(kN_r\theta)\} \quad (14)$$

$$L_{sa1} = L_{sa2} = 2N_b^2\{A\ln(\frac{cr}{3l_0}+1)+\frac{B}{l_0} + [C\ln(\frac{cr}{3l_0}+1)+\frac{D}{l_0}]\sum_{k=1}^{\infty}\frac{\sin^2(\frac{\pi kN_r}{24})}{k^2}\cos(kN_r\theta)\} \quad (15)$$

$$M_{(ma,sa1)} = 2N_m N_b\{A\ln(\frac{\frac{cr}{3}\alpha}{\frac{cr}{3}l_0+l_0^2}+1)+\frac{B\alpha}{l_0^2} + [C\ln(\frac{\frac{cr}{3}\alpha}{\frac{cr}{3}l_0+l_0^2}+1)+\frac{D\alpha}{l_0^2}]\sum_{k=1}^{\infty}\frac{\sin^2(\frac{\pi kN_r}{24})}{k^2}\cos(kN_r\theta)\} \quad (16)$$

$$M_{(ma,sa2)} = 2N_m N_b\{A\ln(\frac{\frac{cr}{3}\beta}{\frac{cr}{3}l_0+l_0^2}+1)+\frac{B\beta}{l_0^2} + [C\ln(\frac{\frac{cr}{3}\beta}{\frac{cr}{3}l_0+l_0^2}+1)+\frac{D\beta}{l_0^2}]\sum_{k=1}^{\infty}\frac{\sin^2(\frac{\pi kN_r}{24})}{k^2}\cos(kN_r\theta)\} \quad (17)$$

$$M_{(sa1,sa2)} = 0 \quad (18)$$

Finite Element Analysis

Finite element method was applied to the calculation of the two-dimensional magnetic field distribution in the cross section to examine the accuracy of the inductances calculated above. ANSYS, a finite element analysis package, is used to calculate inductances of main winding and radial force winding, as shown in Fig.3. Then, FFT is used to analyze the data obtained so that the least terms needed to sum can be decided. Fig.4 shows that summing 3 terms (k=1,2) works well. Fig.5 illustrates self-inductance of both main winding and radial force winding, using

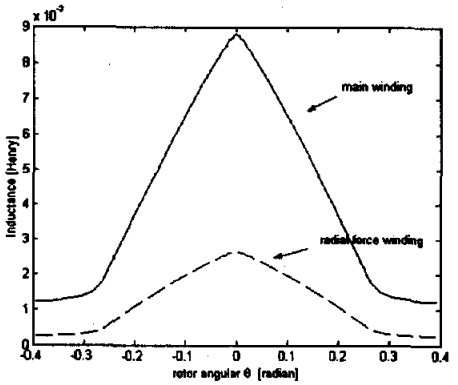

FIGURE.3: Self inductance of the main winding and radial force winding

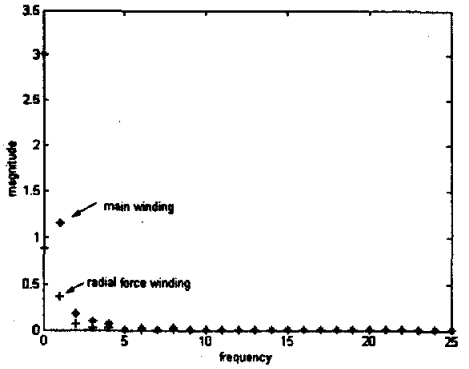

FIGURE.4: FFT of main winding and radial force winding

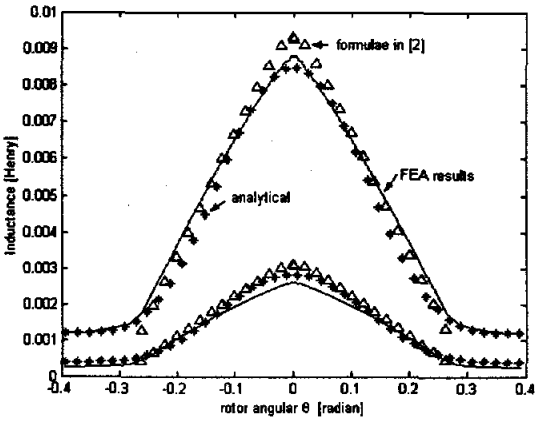

FIGURE.5: Comparison of self-inductance of main winding and radial force winding

formulae in [2] and new formulae discussed in this paper. FEA result is also shown in this figure, so that the results can be compared. It should be noticed that inductance calculated in [2] is from –15 degree to 15

degree, while FEA and formulae presented in this paper are from –22.5 degree to 22.5 degree. It is observed that values obtained using (14) and (15) predicts well with values got in [2].

DERIVATION OF RADIAL FORCES

From the self-inductances and mutual inductances derived above, the stored magnetic energy can be written as,

$$W_a = \frac{1}{2}[i_{ma} \quad i_{sa1} \quad i_{sa2}][L]\begin{bmatrix} i_{ma} \\ i_{sa1} \\ i_{sa2} \end{bmatrix} \tag{19}$$

Where the L is,

$$[L] = \begin{bmatrix} L_{ma} & M_{(ma,sa1)} & M_{(ma,sa2)} \\ M_{(ma,sa1)} & L_{sa1} & M_{(sa1,sa2)} \\ M_{(ma,sa2)} & M_{(sa1,sa2)} & L_{sa2} \end{bmatrix} \tag{20}$$

Thus the radial forces can be written as,

$$F_\alpha = \frac{\partial W}{\partial \alpha} = 2N_m N_b i_{ma} i_{sa1} \{\frac{Acr}{cr(\alpha + l_0) + 3l_0^2} + \frac{B}{l_0^2} + [\frac{Ccr}{cr(\alpha + l_0) + 3l_0^2} + \frac{D}{l_0^2}] \bullet \sum_{k=1}^{2} \frac{\sin^2(\frac{\pi k N_r}{24})}{k^2} \cos(kN_r\theta)\} \tag{21}$$

$$F_\beta = \frac{\partial W}{\partial \beta} = 2N_m N_b i_{ma} i_{sa2} \{\frac{Acr}{cr(\beta + l_0) + 3l_0^2} + \frac{B}{l_0^2} + [\frac{Ccr}{cr(\beta + l_0) + 3l_0^2} + \frac{D}{l_0^2}] \bullet \sum_{k=1}^{2} \frac{\sin^2(\frac{\pi k N_r}{24})}{k^2} \cos(kN_r\theta)\} \tag{22}$$

It is observed that values obtained using (21) predicts well with values got in [2]. But the discrepancy between FEA results and the two theoretical values is not negligible in the aligned region. To improve the accuracy of analytical expression of the rotor position θ_1 and θ_2 will help to improve the accuracy of the value of radial force. As rotor position has been stably controlled using model developed in [2], (21) and (22) is also expected to be effective. Work is proceeding on the construction of this motor, experimental results are expected in the near future.

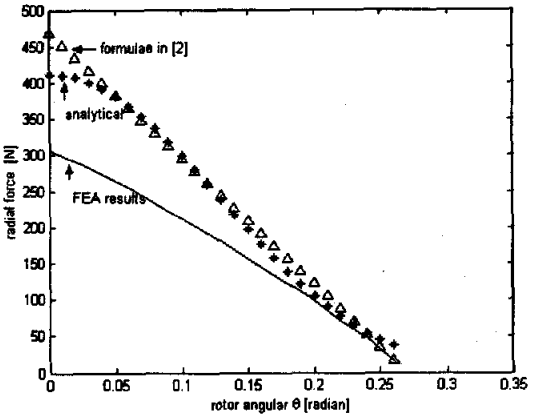

FIGURE.6: Comparison of F_α@ i_{ma}=10A i_{sa1}=3A i_{sa2}=3A

CONCLUSION

In this paper, two main winding modes are compared NSNS mode is found to be more preferable. New formulae for radial forces based on Fourier analysis of the permeance have been proposed. Expression obtained through Fourier extension is differentiable and is also effective in general switched reluctance motors supported by mechanical bearings.

References

1. Eike Richter and Caio Frreira, "Performance Evaluation of a 250kW Switched Reluctance Starter Generator", IEEE IAS'95, pp.434-440, 1995

2. M. Takemoto, K.Shimada, A. Chiba, "A Design and Characteristics of Switched Reluctance Type Bearingless Motors," in *Proc.4th Int. Symp. Magnetic Suspension Technology*, vol.NASA/CP-1998-207654, May 1998,pp.49-63

3. M. Takemoto, A. Chiba,T.Fkao, "A Method of Determining Advanced Angle of Square-wave Currents in Bearingless Switched Reluctance Motors" IEEE Trans Ind. Applicat., vol.37, pp.1702-1709,

NO.6 2001.

4. Liu Chuang "Theoretical study and Engineering Practice on Switched Reluctance Starter/Generator system" a Dissertation for Ph.D. Nanjing University of Aeronautics and Astronautics, Nanjing, P.R.C

SUPPLEMENT

$$A = \frac{4\mu_0 h}{\pi}(1 - \frac{N_r}{24})$$

$$B = \frac{2\pi N_r \mu_0 hr}{24^2}$$

$$C = \frac{-8\mu_0 h}{N_r}\frac{24}{\pi^3}$$

$$D = \frac{4\mu_0 hr}{N_r \pi}$$